Stevenson, N. K. and Brown, C. T. A. and Hopkins, J.-M. and Dawson, M. D. and Kränkel, C. and Lagatsky, A. A. (2018) Diode-pumped femtosecond Tm3+-doped LuScO3 laser near 2.1 µm. Optics Letters, 43 (6). pp. 1287-1290. ISSN 0146-9592 , http://dx.doi.org/10.1364/OL.43.001287

Title: Diode-pumped femtosecond Tm3+-doped LuScO laser near 2.1 m

Authors: Neil Stevenson,Tom Brown,John-Mark Hopkins,Martin D. Dawson,Christian Kraenkel,Alex

Accepted: 14 February 18
Posted 15 February 18
Doc. ID: 309226

Diode-pumped femtosecond Tm^{3+}-doped $LuScO_3$ laser near 2.1 µm

N. K. STEVENSON,[1,2,*] C. T. A. BROWN,[2] J. -M. HOPKINS,[1] M. D. DAWSON,[1,3] C. KRÄNKEL,[4,5] AND A. A. LAGATSKY[1]

[1]Fraunhofer Centre for Applied Photonics, Fraunhofer UK, Technology and Innovation Centre, Glasgow, G1 1RD, UK
[2]SUPA, School of Physics and Astronomy, University of St Andrews, St Andrews, KY16 9SS, UK
[3]Institute of Photonics, University of Strathclyde, Technology and Innovation Centre, Glasgow G1 1RD, UK
[4]Zentrum für Lasermaterialien, Leibniz-Institute for Crystal Growth, Max-Born-Straße 2, 12489 Berlin, Germany
[5]Institut für Laser-Physik, Universität Hamburg, Luruper Chaussee 149, 22769 Hamburg, Germany
*Corresponding author: neil.stevenson@fraunhofer.co.uk

Received XX Month XXXX; revised XX Month, XXXX; accepted XX Month XXXX; posted XX Month XXXX (Doc. ID XXXXX); published XX Month XXXX

We report on the first demonstration of a diode-pumped Tm:LuScO$_3$ laser. Efficient and broadly tunable continuous wave operation in the 1973 – 2141 nm region and femtosecond mode-locking through the use of an ion-implanted InGaAsSb quantum-well-based SESAM are realized. When mode-locked, near transform limited pulses as short as 170 fs were generated at 2093 nm with an average output power of 113 mW and a pulse repetition frequency of 115.2 MHz. Tunable picosecond pulse generation was demonstrated in the 2074 – 2104 nm spectral range.

OCIS codes: *(140.7090) Ultrafast lasers; (140.4050) Mode-locked lasers; (140.5680) Rare earth and transition metal solid-state lasers (140.3070) Infrared and far-infrared lasers.*

http://dx.doi.org/xxxxxxxxxxxxxxxxxxxxxxxxxxxxxxxxxxxxxxxxxxxxxxxx

The development of efficient, low-cost and robust ultrashort pulse lasers in the ~ 2 – 2.1 µm spectral region is required for many application areas in the mid-infrared (mid-IR) photonics sector [1]. In particular, such high peak power lasers can be used to efficiently access the deeper mid-IR region through optical parametric frequency conversion techniques, utilizing nonlinear crystals such as ZGP [2] and OP-GaAs [3], or supercontinuum generation in highly nonlinear fibers [4]. Such mid-IR frequency comb systems [5] are of particular interest for high precision spectroscopy [6], environmental monitoring [7], and medical diagnostics [8]. Compact and efficient ultrafast 2 µm lasers can also be used as seed sources for developing high energy amplifier systems operating in the ~ 2 – 7 µm region [9] which will benefit many applications from the areas of pulsed laser deposition [10] and strong-field physics [11], as well as the development of tabletop X-ray coherent sources [12] and minimally invasive surgery [13].

Tm^{3+}-doped and Tm^{3+}, Ho^{3+}-codoped gain media are excellent candidates for the development of high-power, broadly tunable and compact lasers in the 1.9 – 2.1 µm region due to their ability to be diode-pumped at around 800 nm while the presence of efficient cross relaxation energy transfer processes increase laser quantum efficiency.

Tm^{3+}-doped cubic sesquioxides RE_2O_3 (RE=Lu, Sc, Y, or any $Lu_aSc_bY_c$ composition, where $a + b + c = 1$) occupy a prominent position amongst other Tm^{3+}-doped gain media. They possess advantageous thermo-mechanical properties and spectroscopic features that make them ideal for high power lasers development in the 2 – 2.1 µm region [14]. In contrast to most Tm^{3+}-doped crystalline and amorphous gain media, their broadband emission spectra extend well beyond 2 µm allowing efficient femtosecond pulse operation close to 2.1 µm. Previously, Tm^{3+}-doped Lu_2O_3 in the form of crystals and ceramics have generated sub-200 fs pulses near 2070 nm through the use of a single-walled carbon nanotube saturable absorber [15] and an InGaAsSb quantum-well-based semiconductor saturable absorber mirror (SESAM) [16]. Pulses as short as 218 fs and 166 fs at around 2100 nm were produced with Tm:Sc_2O_3 crystals employing SESAM or Kerr-lens mode-locking techniques, respectively [17,18]. Further reduction of pulse duration was realized using Tm^{3+}-doped mixed sesquioxide host $LuScO_3$ which combines the optical properties of Tm:Lu_2O_3 and Tm:Sc_2O_3 resulting in a broad, smooth and relatively flat gain spectrum extending from 1.95 µm to 2.15 µm [19]. While the lower thermal conductivity of $LuScO_3$ (3.9 W/(m·K) [19]), compared to other sesquioxides, could limit its use for high power operation, the benefits the host brings in terms of its spectroscopic properties for ultrashort pulse generation are indispensable. Indeed, a mode-locked (ML) Tm:$LuScO_3$ crystalline laser [20] has demonstrated a 105 fs pulse duration and, more recently, pulses as short as 63 fs were generated with an output power of 34 mW from a Tm:$LuScO_3$ mixed ceramic laser [21]. However, it should be highlighted that all the above achievements were realized using high beam quality Ti:sapphire lasers or Er:Yb fiber MOPA as pump sources. Such pump sources are expensive, bulky, offer limited pump powers and represent a major obstacle towards development of practical ultrafast lasers near the 2 µm region. Commercially available AlGaAs-based laser diodes operating around 800 nm on the other hand offer a considerably more compact and less expensive pump source option capable of higher power operation that can match the main absorption wavelengths of Tm^{3+}-doped laser crystals. However, the development of a diode-pumped ultrafast Tm^{3+}-doped laser is not a trivial task due to poor pump beam quality resulting in a lower efficiency, higher thermal load, Q-switching instabilities, and weaker self-phase modulation inside the gain medium. Indeed, the range of diode-pumped mode-locked Tm^{3+}-doped lasers reported to date is rather limited with only a few demonstrations of sub-picosecond operation (Fig. 1). Recently we reported a diode-pumped $Tm:Lu_2O_3$ ceramic laser producing 240 fs pulses with an average power of up to 500 mW [22]. Combining the unique optical properties of the $Tm:LuScO_3$ gain medium with a compact and efficient laser diode pump configuration will allow the realization of low-cost and practical femtosecond lasers, broadly tunable in the 2 – 2.1 µm wavelength range suitable for many mid-IR application areas including seeding of existing Tm and Ho amplifier systems.

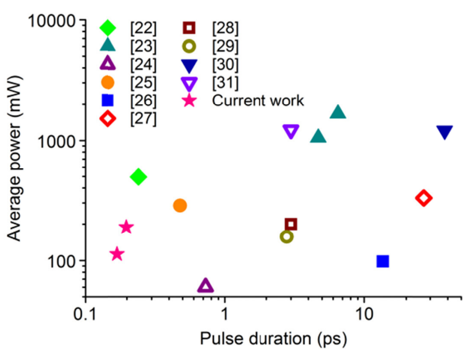

Fig. 1. State-of-the-art performance summary of diode-pumped mode-locked Tm^{3+}-doped solid-state lasers in the ~ 2 – 2.1 µm spectral region [22–31].

Here we report, for the first time to our knowledge, a diode-pumped, passively ML $Tm:LuScO_3$ laser. Near transform-limited pulses as short as 170 fs were generated at a center wavelength of 2093 nm with an average output power of 113 mW. In addition, tunable picosecond pulse generation was realized in the 2074 – 2104 nm range. Continuous wave (CW) characterization was also undertaken under direct diode pumping, demonstrating slope efficiencies of up to 33% corresponding to a maximum output power of 660 mW at 2102 nm. In the CW regime a tunable bandwidth of 75 nm at full width at half maximum (FWHM) was recorded highlighting the potential of this medium for the generation of even shorter pulses.

The CW and ML performance of the laser were characterized using a four mirror z-fold cavity design, as shown in Fig. 2. A multimode laser diode (LD) with emitting area of 90 × 1 µm² operating at 793 nm with a maximum output power of 4 W was used as a pump source. The pump beam quality parameter, M^2, was measured to be 17 and 1.2 for *x* and *y* directions, respectively. The pump beam was first collimated in the fast axis by a 3.1 mm focal length aspheric lens (L1) before passing through a pair of cylindrical lenses (L2 and L3; focal lengths of -7.7 mm and 200 mm, respectively) for beam expansion and collimation in the slow axis. The collimated beam was then focused using a 100 mm achromatic doublet lens (L4) to a measured pump waist radii of 43 µm × 23 µm at the position of the gain crystal. The pump beam steering dielectric mirror (SM) was used to minimize the overall set-up footprint. The four mirror laser cavity consisted of a plane-wedged high-reflectivity mirror (HR), two curved mirrors with the radius of curvature of 75 mm (M1 and M2) and a plane-wedged output coupler (OC). A plane-plane, 4 mm long, 3 mm × 3 mm in aperture, antireflection coated, 4 at.% Tm^{3+}-doped $LuScO_3$ (LC) crystal was used for all laser experiments. It was grown by the heat exchanger method in a rhenium crucible as described in [19]. The crystal was mounted onto a heatsink which was maintained at 20 °C by using a thermoelectric cooler device. The laser cavity waist within the laser crystal was calculated to have radii of 24 µm × 21 µm. Apart from the OCs, all cavity mirrors were coated for a high reflectivity at 1900 – 2100 nm and a high transmission at around 800 nm. The OCs had transmissions of 1%, 2%, 4% and 5% between 1900 nm and 2100 nm.

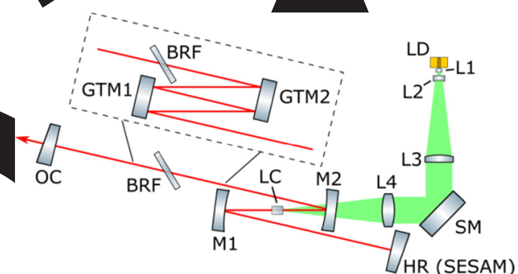

Fig. 2. Experimental setup for CW and ML characterization of the $Tm:LuScO_3$ laser. In ML operation two GTI type mirrors (GTM1 and GTM2) are inserted into the long arm of the cavity and the HR mirror is replaced with a SESAM. BRFs shown were used for tuning in both CW and ML operation.

The maximum CW output power of 660 mW was achieved using a 2% OC with a corresponding slope efficiency of 33% at 2102 nm. A laser threshold of 194 mW of absorbed pump power was measured (Fig. 3(a)). The gain element absorbed about 67% of the pump radiation. It should be noted that further increase in the output coupling resulted in a laser efficiency drop due to presence of up-conversion losses originating from the upper laser level $^3F_4$ of Tm^{3+}. The tunability of the laser was investigated by inserting a 1.6 mm think quartz birefringent filter (BRF) at Brewster's angle into the long arm of the cavity. Using the 2% OC a tuning range of 1973 – 2141 nm was recorded (Fig. 3(b)) with a FWHM bandwidth of 75 nm.

For ML operation the laser cavity was altered so that it operated in stability region II producing a second intracavity beam waist with an average radius of 110 µm on the SESAM without the need for implementation of additional cavity optics. The SESAM device was an ion-implanted InGaAsSb quantum-well-based structure characterized by a low-signal reflection of 99.5-98.1% in the 2 – 2.1 µm range, modulation depth and nonsaturable loss of 1% and

0.9%, respectively, at 2100 nm and a saturation fluence of ~ 50 μJ/cm^2 [32]. The SESAM element was mounted on a brass heatsink maintained at a temperature of 20 °C. Two Gires-Tournois interferometer (GTI) type high-reflectivity mirrors with -500 fs^2 group delay dispersion (GDD) per reflection at 2 – 2.1 μm were inserted into the long arm of the cavity. Two reflections at each mirror introduced a round-trip dispersion of -4000 fs^2. Additionally, a dispersion of around -300 fs^2 was added from the gain medium resulting in a total round-trip GDD of -4300 fs^2 assuming a negligible GDD from the antiresonant Fabry-Perot SESAM structure at around 2100 nm.

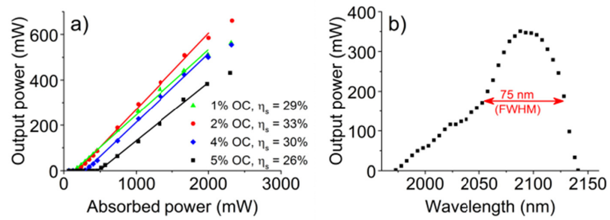

Fig. 3. (a) CW power characteristics for the Tm:LuScO$_3$ laser . (b) The tuning curve achieved from the laser using the 2% OC with the birefringent filter.

ML operation was first demonstrated using the 1% OC. By gradually increasing pump power the self-starting transition between CW and Q-switched ML (QML) operation was observed at an average output power of 49 mW, while the transition to continuous wave single pulse ML (SP-ML) operation was observed at an average output power of 78 mW (Fig. 4(a)). The intracavity laser field fluence on the SESAM at the mode-locking threshold was estimated to be 113 μJ/cm^2. The laser cavity beam waist inside the gain medium was estimated to be 27 μm × 14 μm at such optimized mode-locking conditions. Single pulse operation was maintained up to a maximum average output power of 113 mW. Beyond this point multiple pulse (MP) mode-locking was observed. Near transform limited pulses with duration of 170 fs (assuming a sech^2 intensity autocorrelation profile) were recorded at an average output power of 113 mW (Fig. 4(b)). The corresponding optical spectrum at 2093 nm, seen in Fig. 4(c), had a FWHM of 27.7 nm indicating a time-bandwidth product of 0.32. Stable mode-locked operation was confirmed by the radio frequency (RF) spectrum (Fig. 4(d)) which shows the fundamental beat note at 115.23 MHz with an extinction ratio of 71 dB above the carrier, while a 1 GHz span showed no Q-switching instabilities and a near constant extinction ratio over the harmonic beat notes. Additionally, single pulse operation was monitored by autocorrelation traces with the maximum span of up to 50 ps and mode-locked pulse trains recorded using a high-speed photodetector.

Switching to a 2% OC resulted in a maximum average output power of 190 mW (Fig. 5(a)) during SP-ML limited only by the available pump power. In this case, self-starting QML was observed first at 127 mW of average output power followed by a transition to SP-ML at 171 mW which was maintained up to the maximum generated power of 190 mW where pulses as short as 198 fs were produced (Fig. 5(b)). The threshold for mode-locking was estimated to be at an intracavity fluence on the SESAM of 145 μJ/cm^2. The corresponding optical spectrum was found to center at 2094 nm with a bandwidth of 24 nm (Fig. 5(c)) implying a time-bandwidth product of 0.33. The RF spectrum (Fig. 5(d)) recorded with a span of 200 kHz and resolution bandwidth (RBW) of 200 Hz shows the fundamental beat note at 115.26 MHz with an extinction ratio of 71 dB above the carrier with no Q-switching instabilities observed. The output beam quality of the laser was determined by performing an M^2 measurement using a scanning slit beam profiler in combination with a 75 mm plano-convex lens. The results of the measurements showed a slightly astigmatic focus and M^2 values of 1.1 in both the horizontal and vertical directions.

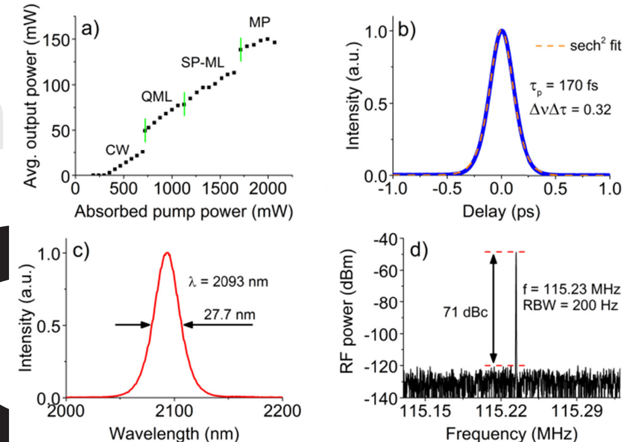

Fig. 4. (a) Power characteristics of the ML Tm:LuScO$_3$ laser with the 1% OC. The autocorrelation trace with sech^2 fit (b), emission spectrum (c), and 200 kHz span RF spectrum (d) for a 170 fs pulse at 113 mW average output power.

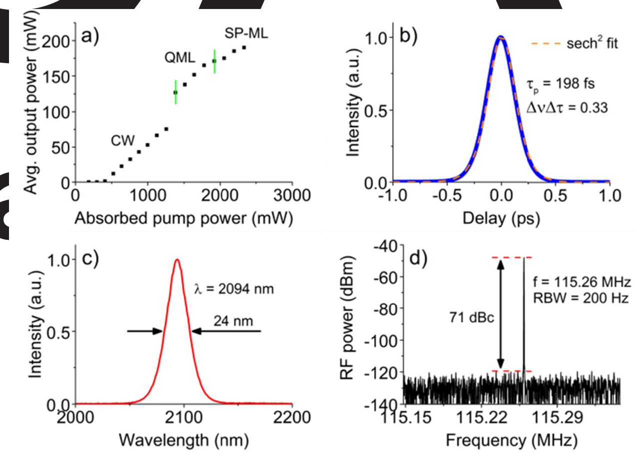

Fig. 5. (a) Power characteristics for ML operation with the 2% OC. The autocorrelation trace with sech^2 fit (b), emission spectrum (c), and 200 kHz span RF spectrum (d) for a 198 fs pulse at 190 mW.

Tunability of the ML Tm:LuScO$_3$ laser was investigated using a 1.6 mm thick quartz BRF (Fig. 2) with the 1% OC and at 1.7 W of incident pump power (1.1 W of absorbed power). Tunable picosecond pulses were recorded in the range of 2074 – 2104 nm

(Fig. 6(a)) with the maximum output power of 55.4 mW around 2090 nm. For wavelengths shorter than 2088 nm QML behavior was observed while stable ML operation was observed for wavelengths longer than 2088 nm and up to 2104 nm. The autocorrelation trace and optical spectrum for the laser tuned to 2094 nm can be found in Fig. 6(b) and Fig. 6(c), respectively, indicating the generation of slightly chirped 2.06 ps pulses. It is believed that due to the strong spectral filtering of the BRF the laser operated in non-soliton mode-locking regime and at such conditions the pulse duration was dictated by the relaxation dynamic of SESAM.

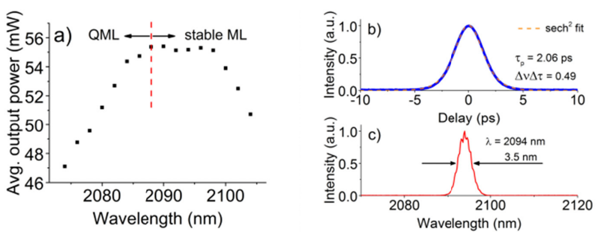

Fig. 6. (a) Tunability of the $Tm:LuScO_3$ laser during ML operation. An autocorrelation trace and optical spectrum for the laser tuned to 2094 nm are shown in (b) and (c) respectively.

In conclusion, we have demonstrated, for the first time to our knowledge, a diode-pumped $Tm:LuScO_3$ laser. During initial CW characterization a maximum output power of 660 mW was generated with the corresponding slope efficiency of 33% at 2102 nm. A tunability range of 1973 – 2141 nm was demonstrated. When mode-locked, near transform-limited pulses as short as 170 fs with an average output of 113 mW at 2093 nm have been generated. This represents the shortest pulse duration achieved from any diode-pumped Tm laser in the 2 – 2.1 µm region. Under different output coupling conditions, a higher average output power of 190 mW was achieved with the pulse duration of 198 fs at 2094 nm. Tunable picosecond pulse operation has also been demonstrated in the range of 2074 – 2104 nm. With the performance reported in this work, there is potential for this source to be developed into an overall compact and efficient seed laser for further amplification and spectral broadening deeper into the mid-infrared region.

Funding. This work was funded by the UK Engineering and Physical Sciences Research Council (EPSRC) (EP/L01596X/1).

Acknowledgement. Neil K. Stevenson acknowledges the EPSRC Centre for Doctoral Training in Applied Photonics and Fraunhofer UK for studentship funding. The research data supporting this publication can be accessed at http://dx.doi.org/10.17630/198f360d-3b1d-4b83-933c-5608ef15457e.

REFERENCES

1. H. Pires, M. Baudisch, D. Sanchez, M. Hemmer, and J. Biegert, Prog. Quantum Electron. **43**, 1 (2015).
2. P. A. Budni, L. A. Pomeranz, M. L. Lemons, C. A. Miller, J. R. Mosto, and E. P. Chicklis, J. Opt. Soc. Am. B **17**, 723 (2000).
3. N. Leindecker, A. Marandi, R. L. Byer, K. L. Vodopyanov, J. Jiang, I. Hartl, M. Fermann, and P. G. Schunemann, Opt. Express **20**, 7046 (2012).
4. J. Swiderski, Prog. Quantum Electron. **38**, 189 (2014).
5. A. Schliesser, N. Picqué, and T. W. Hänsch, Nat. Photonics **6**, 440 (2012).
6. K. C. Cossel, E. M. Waxman, I. A. Finneran, G. A. Blake, J. Ye, and N. R. Newbury, J. Opt. Soc. Am. B **34**, 104 (2017).
7. G. B. Rieker, F. R. Giorgetta, W. C. Swann, J. Kofler, a M. Zolot, L. C. Sinclair, E. Baumann, C. Cromer, G. Petron, C. Sweeney, P. P. Tans, I. Coddington, and N. R. Newbury, Optica **1**, 290 (2014).
8. F. Adler, M. J. Thorpe, and K. C. Cossel, Annu. Rev. Anal. Chem. **3**, 175 (2010).
9. L. von Grafenstein, M. Bock, U. Griebner, and T. Elsaesser, Opt. Express **23**, 14744 (2015).
10. D. M. Bubb, M. R. Papantonakis, J. S. Horwitz, R. F. Haglund, B. Toftmann, R. A. McGill, and D. B. Chrisey, Chem. Phys. Lett. **352**, 135 (2002).
11. B. Wolter, M. G. Pullen, M. Baudisch, M. Sclafani, M. Hemmer, A. Senftleben, C. D. Schröter, J. Ullrich, R. Moshammer, and J. Biegert, Phys. Rev. X **5**, 1 (2015).
12. T. Popmintchev, M.-C. Chen, D. Popmintchev, P. Arpin, S. Brown, S. Alisauskas, G. Andriukaitis, T. Balciunas, O. D. Mücke, A. Pugzlys, A. Baltuska, B. Shim, S. E. Schrauth, A. Gaeta, C. Hernandez-Garcia, L. Plaja, A. Becker, A. Jaron-Becker, M. M. Murnane, and H. C. Kapteyn, Science (80-.). **336**, 1287 (2012).
13. S. Amini-Nik, D. Kraemer, M. L. Cowan, K. Gunaratne, P. Nadesan, B. A. Alman, and R. J. D. Miller, PLoS One **5**, e13053 (2010).
14. C. Kränkel, IEEE J. Sel. Top. Quantum Electron. **21**, 250 (2015).
15. A. Schmidt, P. Koopmann, G. Huber, P. Fuhrberg, S. Y. Choi, D. Yeom, F. Rotermund, V. Petrov, and U. Griebner, Opt. Express **20**, 5313 (2012).
16. A. A. Lagatsky, O. L. Antipov, and W. Sibbett, Opt. Express **20**, 19349 (2012).
17. A. A. Lagatsky, P. Koopmann, P. Fuhrberg, G. Huber, C. T. A. Brown, and W. Sibbett, Opt. Lett. **37**, 437 (2012).
18. M. Tokurakawa, E. Fujita, and C. Kränkel, Opt. Lett. **42**, 3185 (2017).
19. P. Koopmann, PhD-thesis, University of Hamburg (2012).
20. A. A. Lagatsky, P. Koopmann, O. L. Antipov, C. T. A. Brown, G. Huber, and W. Sibbett, in *2013 Conference on Lasers & Electro-Optics Europe & International Quantum Electronics Conference CLEO EUROPE/IQEC* (IEEE, 2013), pp. 1–1.
21. Y. Wang, W. Jing, P. Loiko, Y. Zhao, H. Huang, S. Suomalainen, A. Härkönen, M. Guina, X. Mateos, U. Griebner, and V. Petrov, in *Laser Congress 2017 (ASSL, LAC)* (OSA, 2017), p. ATu6A.4.
22. A. A. Lagatsky and J.-M. Hopkins, in *Laser Congress 2016 (ASSL, LSC, LAC)* (2016), p. JTu2A.5.
23. H. Cheng, X. D. Jiang, X. P. Hu, M. L. Zhong, X. J. Lv, and S. N. Zhu, Opt. Lett. **39**, 2187 (2014).
24. J. Ma, G. Q. Xie, P. Lv, W. L. Gao, P. Yuan, L. J. Qian, H. H. Yu, H. J. Zhang, J. Y. Wang, and D. Y. Tang, Opt. Lett. **37**, 2085 (2012).
25. J. Ma, G. Q. Xie, W. L. Gao, P. Yuan, L. J. Qian, H. H. Yu, H. J. Zhang, and J. Y. Wang, Opt. Lett. **37**, 1376 (2012).
26. C. Luan, K. Yang, J. Zhao, S. Zhao, T. Li, H. Zhang, J. He, L. Song, T. Dekorsy, M. Guina, and L. Zheng, Opt. Lett. **42**, 839 (2017).
27. Z. Qin, G. Xie, L. Kong, P. Yuan, L. Qian, X. Xu, and J. Xu, IEEE Photonics J. **7**, 1 (2015).
28. M. Gaponenko, V. J. Wittwer, A. Härkönen, S. Suomalainen, N. Kuleshov, M. Guina, and T. Südmeyer, Opt. Express **25**, 25760 (2017).
29. J. Ma, G. Xie, J. Zhang, P. Yuan, D. Tang, and L. Qian, IEEE J. Sel. Top. Quantum Electron. **21**, (2015).
30. T. Feng, K. Yang, J. Zhao, S. Zhao, W. Qiao, T. Li, T. Dekorsy, J. He, L. Zheng, Q. Wang, X. Xu, L. Su, and J. Xu, Opt. Express **23**, 11819 (2015).
31. C. Y. Cho, Y. F. Chen, G. Zhang, W. D. Chen, and H. C. Liang, Opt. Lett. **42**, 5226 (2017).
32. A. A. Lagatsky, X. Han, M. D. Serrano, C. Cascales, C. Zaldo, S. Calvez, M. D. Dawson, J. A. Gupta, C. T. A. Brown, and W. Sibbett, Opt. Lett. **35**, 3027 (2010).

1. H. Pires, M. Baudisch, D. Sanchez, M. Hemmer, and J. Biegert, "Ultrashort pulse generation in the mid-IR," Prog. Quantum Electron. **43**, 1–30 (2015).
2. P. A. Budni, L. A. Pomeranz, M. L. Lemons, C. A. Miller, J. R. Mosto, and E. P. Chicklis, "Efficient mid-infrared laser using 19-μm-pumped Ho:YAG and ZnGeP_2 optical parametric oscillators," J. Opt. Soc. Am. B **17**, 723 (2000).
3. N. Leindecker, A. Marandi, R. L. Byer, K. L. Vodopyanov, J. Jiang, I. Hartl, M. Fermann, and P. G. Schunemann, "Octave-spanning ultrafast OPO with 2.6-6.1μm instantaneous bandwidth pumped by femtosecond Tm-fiber laser," Opt. Express **20**, 7046 (2012).
4. J. Swiderski, "High-power mid-infrared supercontinuum sources: Current status and future perspectives," Prog. Quantum Electron. **38**, 189–235 (2014).
5. A. Schliesser, N. Picqué, and T. W. Hänsch, "Mid-infrared frequency combs," Nat. Photonics **6**, 440–449 (2012).
6. K. C. Cossel, E. M. Waxman, I. A. Finneran, G. A. Blake, J. Ye, and N. R. Newbury, "Gas-phase broadband spectroscopy using active sources: progress, status, and applications [Invited]," J. Opt. Soc. Am. B **34**, 104 (2017).
7. G. B. Rieker, F. R. Giorgetta, W. C. Swann, J. Kofler, a M. Zolot, L. C. Sinclair, E. Baumann, C. Cromer, G. Petron, C. Sweeney, P. P. Tans, I. Coddington, and N. R. Newbury, "Frequency-comb-based remote sensing of greenhouse gases over kilometer air paths," Optica **1**, 290 (2014).
8. F. Adler, M. J. Thorpe, and K. C. Cossel, "Cavity-Enhanced Direct Frequency Comb Spectroscopy : Technology and Applications," Annu. Rev. Anal. Chem. **3**, 175–205 (2010).
9. L. von Grafenstein, M. Bock, U. Griebner, and T. Elsaesser, "High-energy multi-kilohertz Ho-doped regenerative amplifiers around 2 μm," Opt. Express **23**, 14744 (2015).
10. D. M. Bubb, M. R. Papantonakis, J. S. Horwitz, R. F. Haglund, B. Toftmann, R. A. McGill, and D. B. Chrisey, "Vapor deposition of polystyrene thin films by intense laser vibrational excitation," Chem. Phys. Lett. **352**, 135–139 (2002).
11. B. Wolter, M. G. Pullen, M. Baudisch, M. Sclafani, M. Hemmer, A. Senftleben, C. D. Schröter, J. Ullrich, R. Moshammer, and J. Biegert, "Strong-field physics with Mid-IR fields," Phys. Rev. X **5**, 1–16 (2015).
12. T. Popmintchev, M.-C. Chen, D. Popmintchev, P. Arpin, S. Brown, S. Alisauskas, G. Andriukaitis, T. Balciunas, O. D. Mücke, A. Pugzlys, A. Baltuska, B. Shim, S. E. Schrauth, A. Gaeta, C. Hernandez-Garcia, L. Plaja, A. Becker, A. Jaron-Becker, M. M. Murnane, and H. C. Kapteyn, "Bright Coherent Ultrahigh Harmonics in the keV X-ray Regime from Mid-Infrared Femtosecond Lasers," Science (80-.). **336**, 1287–1291 (2012).
13. S. Amini-Nik, D. Kraemer, M. L. Cowan, K. Gunaratne, P. Nadesan, B. A. Alman, and R. J. D. Miller, "Ultrafast Mid-IR Laser Scalpel: Protein Signals of the Fundamental Limits to Minimally Invasive Surgery," PLoS One **5**, e13053 (2010).
14. C. Kränkel, "Rare-Earth-Doped Sesquioxides for Diode-Pumped High-Power Lasers in the 1-, 2-, and 3-um Spectral Range," IEEE J. Sel. Top. Quantum Electron. **21**, 250–262 (2015).
15. A. Schmidt, P. Koopmann, G. Huber, P. Fuhrberg, S. Y. Choi, D. Yeom, F. Rotermund, V. Petrov, and U. Griebner, "175 fs Tm:Lu2O3 laser at 2.07 μm mode-locked using single-walled carbon nanotubes," Opt. Express **20**, 5313 (2012).
16. A. A. Lagatsky, O. L. Antipov, and W. Sibbett, "Broadly tunable femtosecond Tm:Lu_2O_3 ceramic laser operating around 2070 nm," Opt. Express **20**, 19349 (2012).
17. A. A. Lagatsky, P. Koopmann, P. Fuhrberg, G. Huber, C. T. a Brown, and W. Sibbett, "Passively mode locked femtosecond Tm:Sc2O3 laser at 2.1 μm," Opt. Lett. **37**, 437–9 (2012).
18. M. Tokurakawa, E. Fujita, and C. Kränkel, "Kerr-lens mode-locked Tm^3+:Sc_2O_3 single-crystal laser in-band pumped by an Er:Yb fiber MOPA at 1611 nm," Opt. Lett. **42**, 3185 (2017).
19. P. Koopmann, "Thulium- and Holmium-Doped Sesquioxides for 2μm Lasers," University of Hamburg (2012).
20. A. A. Lagatsky, P. Koopmann, O. L. Antipov, C. T. A. Brown, G. Huber, and W. Sibbett, "Femtosecond pulse generation with Tm-doped sesquioxides," in *2013 Conference on Lasers & Electro-Optics Europe & International Quantum Electronics Conference CLEO EUROPE/IQEC* (IEEE, 2013), pp. 1–1.
21. Y. Wang, W. Jing, P. Loiko, Y. Zhao, H. Huang, S. Suomalainen, A. Härkönen, M. Guina, X. Mateos, U. Griebner, and V. Petrov, "Sub-10 optical-cycle mode-locked Tm:(Lu_2/3Sc_1/3)_2O_3 mixed ceramic laser at 2057 nm," in *Laser Congress 2017 (ASSL, LAC)* (OSA, 2017), p. ATu6A.4.
22. A. A. Lagatsky and J.-M. Hopkins, "Diode-pumped Femtosecond Tm-doped Lu2O3 Ceramic Laser," in *Laser Congress 2016 (ASSL, LSC, LAC)* (2016), p. JTu2A.5.
23. H. Cheng, X. D. Jiang, X. P. Hu, M. L. Zhong, X. J. Lv, and S. N. Zhu, "Diode-pumped 1988-nm Tm:YAP laser mode-locked by intracavity second-harmonic generation in periodically poled LiNbO_3," Opt. Lett. **39**, 2187 (2014).
24. J. Ma, G. Q. Xie, P. Lv, W. L. Gao, P. Yuan, L. J. Qian, H. H. Yu, H. J. Zhang, J. Y. Wang, and D. Y. Tang, "Graphene mode-locked femtosecond laser at 2 μm wavelength," Opt. Lett. **37**, 2085 (2012).
25. J. Ma, G. Q. Xie, W. L. Gao, P. Yuan, L. J. Qian, H. H. Yu, H. J. Zhang, and J. Y. Wang, "Diode-pumped mode-locked femtosecond Tm:CLNGG disordered crystal laser," Opt. Lett. **37**, 1376 (2012).

26. C. Luan, K. Yang, J. Zhao, S. Zhao, T. Li, H. Zhang, J. He, L. Song, T. Dekorsy, M. Guina, and L. Zheng, "Diode-pumped mode-locked Tm:LuAG laser at 2 µm based on GaSb-SESAM," Opt. Lett. **42**, 839 (2017).
27. Z. Qin, G. Xie, L. Kong, P. Yuan, L. Qian, X. Xu, and J. Xu, "Diode-Pumped Passively Mode-Locked Tm:CaGdAlO4 Laser at 2-µm Wavelength," IEEE Photonics J. **7**, 1–5 (2015).
28. M. Gaponenko, V. J. Wittwer, A. Härkönen, S. Suomalainen, N. Kuleshov, M. Guina, and T. Südmeyer, "Diode-pumped Tm:KY(WO_4)_2 laser passively modelocked with a GaSb-SESAM," Opt. Express **25**, 25760 (2017).
29. J. Ma, G. Xie, J. Zhang, P. Yuan, D. Tang, and L. Qian, "Passively Mode-Locked Tm:YAG Ceramic Laser Based on Graphene," IEEE J. Sel. Top. Quantum Electron. **21**, (2015).
30. T. Feng, K. Yang, J. Zhao, S. Zhao, W. Qiao, T. Li, T. Dekorsy, J. He, L. Zheng, Q. Wang, X. Xu, L. Su, and J. Xu, "1.21 W passively mode-locked Tm:LuAG laser," Opt. Express **23**, 11819 (2015).
31. C. Y. Cho, Y. F. Chen, G. Zhang, W. D. Chen, and H. C. Liang, "Exploring the self-mode locking of the 2 µm Tm:YAG laser with suppression of the self-pulsing dynamic," Opt. Lett. **42**, 5226 (2017).
32. A. A. Lagatsky, X. Han, M. D. Serrano, C. Cascales, C. Zaldo, S. Calvez, M. D. Dawson, J. A. Gupta, C. T. A. Brown, and W. Sibbett, "Femtosecond (191 fs) NaY(WO4)2 Tm,Ho-codoped laser at 2060 nm," Opt. Lett. **35**, 3027–9 (2010).